Sains Malaysiana 55(2)(2026): 293-304
http://doi.org/10.17576/jsm-2026-5502-09

Controlling the Hydrothermal Reaction and Unlocking the Potential of Porous Substrates for Enhanced Photoelectrochemical Activity in ZnO on Graphene/Nickel Foam

(Mengawal Tindak Balas Hidroterma dan Membuka Potensi Substrat Berliang untuk Peningkatan Aktiviti Fotoelektrokimia dalam ZnO pada Busa Grafin/Nikel)

NUR RABIATUL ADAWIYAH MOHD SHAH[1], NURUL NABILA ROSMAN[2], MOHAMAD AZUWA MOHAMED[1,3,4], KHUZAIMAH ARIFIN[5], LORNA JEFFERY MINGGU[1], WAI YIN WONG[1] & ROZAN MOHAMAD YUNUS[1,*]

[1]Fuel Cell Institute, Universiti Kebangsaan Malaysia, 43600 UKM Bangi, Selangor, Malaysia
[2]Department of Chemistry, Faculty of Science, Universiti Teknologi Malaysia, 81310 UTM Johor Bahru, Johor, Malaysia
[3]Department of Chemical Sciences, Faculty of Science and Technology, Universiti Kebangsaan Malaysia, 43600 UKM Bangi, Selangor, Malaysia
[4]Polymer Research Centre (PORCE), Faculty of Science and Technology, Universiti Kebangsaan Malaysia, 43600 UKM Bangi, Selangor, Malaysia
[5]National Research and Innovation Agency (BRIN), Research Center for Advanced Materials, Building 224, KST BJ Habibie, South Tangerang 15314, Banten, Indonesia

Received: 4 September 2025/Accepted: 27 January 2026

ABSTRACT

Zinc oxide (ZnO) is a promising photoanode material for photoelectrochemical (PEC) applications; however, its limitations, including a wide band gap and a high electron–hole recombination rate, hinder its performance. This study addresses these challenges by growing ZnO on graphene/nickel foam (Gr/Ni-foam) using a hydrothermal method, varying reaction parameters (time: 2, 4, 6, 8, 10 h; temperature: 150, 180 and 200 ºC). Results demonstrate significantly enhanced PEC activity via hydrothermal reaction temperature at 200 ºC for 8 h, attributed to the porous Ni-foam substrate, which improves electrolyte accessibility and light harvesting. Gr further reduces by about 50% the photocurrent onset potential, which in turn boosts charge transfer. Interestingly, ZnO on Gr/Ni-foam exhibits outstanding PEC activity (24.93 mA cm^{-2} at 1.23 V vs RHE) compared to other tested substrates, primarily due to the advantages of the porous structure of Ni-foam. This research highlights the critical role of substrate selection, particularly the use of porous Ni-foam, in overcoming the intrinsic limitations of ZnO to enabling the development of high-performance photoelectrodes for efficient PEC water splitting.

Keywords: Graphene; nickel foam; photoelectrochemical activity; porous substrate; zinc oxide

ABSTRAK

Zink oksida (ZnO) adalah bahan fotoanod yang berpotensi dalam aplikasi fotoelektrokimia (PEC), tetapi prestasinya agak terhad disebabkan oleh beberapa kelemahan seperti sela jalur lebar dan kadar penggabungan semula pasangan elektron-lohong yang pantas. Untuk menangani isu yang dinyatakan, kajian ini menumbuhkan ZnO di atas grafin/busa nikel (Gr/Busa Ni) menggunakan kaedah hidroterma dengan mengubah parameter tindak balas (masa: 2, 4, 6, 8, 10 jam; suhu: 150, 180, 200 ºC). Keputusan menunjukkan peningkatan aktiviti PEC yang ketara menggunakan tindak balas hidroterma pada suhu 200 ºC selama 8 jam yang disebabkan oleh substrat Busa Ni yang berliang dan ia meningkatkan kebolehcapaian elektrolit dan penyerapan cahaya. Kehadiran Gr mengurangkan keupayaan *onset* fotoarus sebanyak 50% dan menyebabkan berlaku pemindahan cas yang lebih cekap. Menariknya, ZnO pada Gr/Busa Ni menunjukkan aktiviti PEC yang tinggi (24.93 mA cm^{-2} pada 1.23 V vs RHE) berbanding dengan substrat yang lain disebabkan oleh kelebihan struktur Busa Ni yang berliang. Penyelidikan ini menekankan kepentingan pemilihan Busa Ni berliang sebagai substrat fotoelektrod bagi mengatasi batasan intrinsik ZnO, seterusnya membolehkan pembangunan fotoelektrod yang berpestasi tinggi untuk pembelahan molekul air yang cekap melalui PEC.

Kata kunci: Aktiviti fotoelektrokimia; busa nikel; grafin; substrat berliang; zink oksida

INTRODUCTION

Global warming occurs because carbon dioxide, methane, nitrous oxide, chlorofluorocarbons, and tropospheric ozone enable shortwave radiation from the sun to penetrate the atmosphere and warm the Earth's surface. Therefore, renewable energy is required to prevent global warming, in addition to an alternative source of clean and sustainable energy, such as hydrogen (H_2). Many methods for producing H_2 have been established, but the photoelectrochemical (PEC) water splitting is promising because of its simple and direct process for water splitting, where H_2 is produced from water by using sunlight as an energy source (Dias & Mendes 2019; Megia et al. 2021; Shaker et al. 2024).

Semiconductors have been used as photoelectrodes to split water while absorbing light (Hong et al. 2020; Rosman et al. 2021). Titanium dioxide (TiO_2) is a well-known semiconductor developed by Fujishima and Honda in 1972 (Arifin et al. 2021). Yet lately, zinc oxide (ZnO) has received considerable interest as a substitute for TiO_2 because of the nearly identical band energy properties (3.37 eV and 3.20 eV, respectively). Furthermore, owing to its stable structure, non-toxicity, strong exciton binding energy, ease to synthesis, excellent electric and magnetic properties, and outstanding thermal and mechanical stability, ZnO has a higher light absorption rate in the solar spectrum than TiO_2 (Pruna et al. 2018; Raizada, Sudhaik & Singh 2019; Yusoff et al. 2017). However, the wide band gap of ZnO limits electron transport from the valence band (VB) to the conduction band (CB), resulting in the rapid recombination rate of electron–hole pairs and low PEC performance (Pratomo et al. 2023; Sohaib et al. 2023). Various solutions have been explored, including doping ZnO with metals or non-metals, semiconductor coupling, carbon (C)-based integration, controlling crystal growth, and surface modification (Ong, Ng & Mohammad 2018; Pirhashemi, Habibi-Yangjeh & Rahim Pouran 2018). Among these, coupling with C-based materials is promising, as it enhances charge separation, reduces the band gap, increases light absorption, and improves the stability of ZnO.

Graphene (Gr), a two-dimensional (2D) hexagonal C material with high specific surface area, excellent carrier mobility, outstanding thermal conductivity, strong chemical stability, and high mechanical strength, can serve as an electron sink or co-catalyst to increase the PEC performance of ZnO photoelectrode (Geim & Novoselov 2007; Mohd Shah et al. 2021; Qiu, Xing & Zhang 2018). The photocatalytic performance of ZnO improves in the presence of Gr owing to a synergistic effect between Gr and ZnO (Mahmud et al. 2020; Xu et al. 2011). It can decrease the band gap energy of ZnO after adding Gr and broadening the light absorption range (Gaidi et al. 2018; Mohamed Saheed et al. 2021). Furthermore, the integration of Gr with ZnO can facilitate fast electron transport and efficient electron–hole pairs separation (Effendi et al. 2017). However, 2D Gr tends to aggregate and reduce the PEC performance (Li et al. 2016). Previous studies have shown that growing Gr on an interconnected three-dimensional (3D) network, such as nickel foam (Ni-foam) can increase photocurrent density and result in a high surface area and excellent light absorption (Gadisa et al. 2021; Karimizadeh et al. 2018). This could be ascribed to the porous structure of Ni-foam that offers multiple channels for electron transport and light scattering. A 3D network structure provides an intimate contact between ZnO and Gr (Chen et al. 2015). This study extends beyond conventional ZnO on Gr/Ni-foam composites by investigating the roles of hydrothermal reaction time, temperature, substrate selection, and the synergistic effects on enhancing the PEC performance. By adjusting these parameters, we modify the material properties and employ the advantages of the porous Ni-foam to achieve improved PEC performance.

Several porous materials can be utilised as substrates for photoelectrodes, including metal foams, felts, and cloths. For PEC application, Ni-foam was the preferred substrate due to its superior conductivity, high surface area, and robust support for the active material. Therefore, Ni-foam was employed as a substrate to grow Gr via chemical vapor deposition (CVD) followed by a hydrothermal method for decorating ZnO on Gr/Ni-foam photoelectrode. The effect of hydrothermal parameters for ZnO growth on Gr/Ni-foam has been studied along with Ni-foam- supported PEC activity. A comparative study between Ni-foam and Ni-foil showed that the utilization of Ni-foam as a substrate significantly enhanced PEC performance. As a result, ZnO on Gr/Ni-foam significantly enhanced PEC activity among all samples at 1.23 V vs RHE.

MATERIALS AND METHODS

PREPARATION OF GRAPHENE/NICKEL FOAM (Gr/Ni-FOAM) SUBSTRATE

Gr/Ni-foam was synthesized via the CVD technique (Mohd Shah et al. 2022a), where methane (CH_4) was used as the C source. The center of a quartz tube furnace (50 OD × 44 ID × 450 L in mm) was loaded with a 1.5 cm × 1.5 cm piece of cleaned Ni-foam. To minimize contamination from outside air and oxygen gas, the quartz tube was purged using argon (Ar) gas (Seravalli & Bosi 2021). Then, it was heated to 1000 °C for 50 min in the presence of Ar (100 sccm) and Ar/hydrogen (H_2) (400 sccm) gases, followed by 50 min of annealing. To grow Gr onto the Ni-foam substrate, CH_4 (20 sccm) gas was flowed along with Ar (150 sccm) and Ar/H_2 (250 sccm) for 30 min. The sample was then rapidly cooled from 400 °C in the presence of Ar (500 sccm) before it was taken out from the tube furnace.

PREPARATION OF ZINC OXIDE ON GRAPHENE/NICKEL FOAM (ZnO ON Gr/Ni-FOAM)

Zinc nitrate hexahydrate ($Zn(NO_3)_2.6H_2O$) (0.5 M) was used as a precursor and mixed with 30 mL of deionized (DI) water and stirred for 30 min. The mixture was transferred to a 50 mL Teflon-lined stainless-steel hydrothermal autoclave, and several drops of NaOH (5 M) were added to adjust the pH to 4 before immersing the Gr/Ni-foam (Mohd Shah et al. 2022b). The morphology of ZnO is controlled by varying the reaction time from 2 - 10 h at a constant temperature of 150 °C, labeled as T-2, T-4, T-6, T-8, and T-10. Then, the best reaction time determined from this step was employed for further optimization of the hydrothermal reaction temperatures at 150 °C, 180 °C, and 200 °C, labelled as P-1, P-2, and P-3. All samples prepared were then rinsed with DI water before being heated to 450 °C for 1 h. To investigate the influence on porous substrate in enhancing the PEC activity, ZnO growth on Ni-foil has been carried out under the same conditions as those optimized for Ni-foam, including reaction time and temperature. Figure 1 demonstrates the detailed preparation process.

CHARACTERIZATION

The morphological surface and structure of the photoelectrode were examined with a SUPRA 55VP field emission scanning electron (FESEM) microscope. The structural fingerprint of Gr was measured with a 532 nm laser Thermo Scientific DXR2xi Raman spectrometer. The X-ray diffraction (XRD) patterns ($2\theta = 20 - 80°$) of the ZnO crystal structure were collected using a Bruker D8 Advance X-ray diffractometer.

PHOTOELECTROCHEMICAL (PEC) ACTIVITY MEASUREMENTS

The PEC study was conducted using potentiostat (Ametek Versastat 4) with a three-electrode system attached to a PEC cell. The working electrodes (Ni-foam, Ni-foil, Gr/Ni-foam, Gr/Ni-foil, ZnO on Ni-foam, ZnO on Ni-foil, and ZnO on Gr/Ni-foam) were fixed to 1.5 cm^2 exposed area. The platinum (Pt) wire and silver/silver chloride (Ag/AgCl) saturated in 3 M potassium chloride were used as the counter and reference electrode, respectively. The photocurrent measurements were performed using the linear sweep voltammetry (LSV) function from 0 to 1.0 V vs Ag/AgCl at a scan rate of 0.05 V s^{-1}. The samples were examined in complete darkness and under xenon light illumination (100 mW cm^{-2}) with a solar AM 1.5 filter that imitates sunlight (Moridon et al. 2019). The Nyquist plot was carried out using electrochemical impedance spectroscopy (EIS) with a frequency range of 1 Hz to 100 kHz at 0.6 V vs Ag/AgCl in dark conditions, as this potential exceeds the thermodynamic water-splitting potential (1.23 V vs RHE) (Qian et al. 2021). This selection ensures that the samples operate within the steady-state photocurrent response, allowing for a more accurate evaluation of the charge transfer kinetics compared to the low-bias region. These measurements were performed in 30 mL of 0.5 M sodium sulfite (Na_2SO_3) electrolyte solution, which was constantly purged with nitrogen gas prior to measurements. Each condition was tested with three samples, and the results were averaged. All data was converted to RHE values (Chandrasekaran et al. 2016).

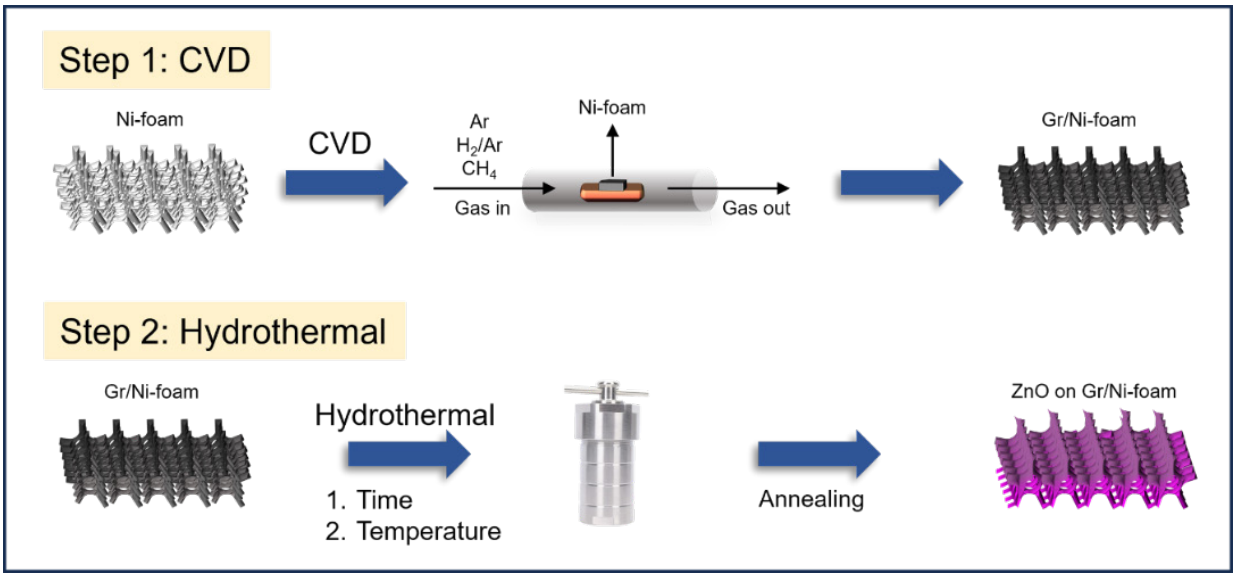

FIGURE 1. Schematic illustration for ZnO on Gr/Ni-foam photoelectrode synthesis via CVD and hydrothermal method

RESULTS AND DISCUSSION

EFFECT OF HYDROTHERMAL REACTION TIME ON ZnO GROWTH OVER Gr/Ni-FOAM SUBSTRATE

Following the successful growth Gr on Ni-foam, ZnO were synthesized on the Gr/Ni-foam substrate using a hydrothermal method at a constant temperature of 150 °C. By systematically varying the reaction time, precise control over the morphology of ZnO was achieved. The hydrothermal reaction time significantly influenced the nucleation and growth kinetics, crystallite size and orientation, surface morphology and coverage area of ZnO on Gr/Ni-foam, thereby impacting the photocatalytic properties and the PEC performance.

From Figure 2(a)-2(e), the ZnO nanostructures exhibit a significant change in surface coverage, as the reaction time increases. At the initial stage (T-2), it is in early stages for ZnO growth, thus the coverage is incomplete (Figure 2(f)). As the reaction time increased from T-4 to T-8, the samples exhibit a significant increase in surface coverage, forming a more compact and uniform flake network that covers the Gr/Ni-foam surface. This results in a hierarchical, interconnected structure that maximizes the active surface area for PEC reactions. However, beyond this temperature (T-10), a decrease in coverage and uniformity is observed, likely due to the depletion of precursor and OH^- ions in the solution, leading to an equilibrium state and limiting further ZnO growth (Zhang et al. 2012). Furthermore, the formation of the nanoflake structure is attributed to the presence of OH-group, which coordinate to stabilize the Zn^{2+} terminated (0001) plane, suppressing c-axis growth caused by the strong charge interaction (Jung & Chu 2014).

To confirm the presence of each element in the sample, XRD measurement was conducted (Figure 2(f)). The broad XRD peak at around 26.44° with PDF 98-001-2084 can be indexed to the (002) plane, which is close to graphitic carbon (Boruah et al. 2015). The intensity of the XRD peaks at 31.72° (010), 34.35° (002), 36.21° (011) and 43.16° (011) can be accurately assigned to ZnO (PDF 98-002-7821). It demonstrates that the samples are well crystallized hexagonal wurtzite-type and highly pure ZnO (Macclesh del Pino Pérez et al. 2019; Men et al. 2016). Besides, three peaks at 44.44°, 51.79°, and 76.32° (PDF 98-006-2897), corresponding to the (111), (002) and (022) planes, respectively, indicate the presence of Ni (Yang et al. 2015). Notably, for the Ni-foam and Gr/Ni-foam samples, a distinct peak at 38.32°, 45.47°, and 65.06°, corresponding to the (111), (111) and (110) plane of NiO (PDF 98-004-9131) were observed, likely resulting from surface oxidation during the annealing process (Nordin et al. 2025). Following ZnO deposition, the peak at 38.32° disappears, which is attributed to the chemical etching of the Ni surface oxide layer within the hydrothermal growth solution. These results confirm the successful growth of ZnO on Gr/Ni-foam substrate through hydrothermal method.

Figure 3(a) depicts the photocurrent curve for all samples. The T-8 sample exhibited a significant increase in photocurrent density, reaching approximately 86.22 mA cm^{-2} at nearly 1 V vs Ag/AgCl, which corresponds to 24.93 mA cm^{-2} at 1.23 V vs RHE. As discussed in the following paragraph, this coverage area and morphological advantage is quantitatively supported by a significant reduction in charge transfer resistance, which facilitates more efficient charge carrier separation compared to the dense or incomplete structures found in the samples. Table 1 presents a comparison of the PEC activity of ZnO with different morphologies. The results demonstrate that the nanoflake ZnO structure exhibits the highest PEC activity among the samples investigated by others. Besides, the addition of Gr together with Ni-foam in ZnO system will enhance the PEC activity (Gadisa, Appiah-Ntiamoah & Kim 2019).

Electrochemical impedance spectroscopy (EIS) was conducted to examine charge transfer, as the efficient charge transfer at sample–electrode interfaces is critical for rapid redox reactions and enhanced the PEC activity. The Nyquist plot in Figure 3(b) shows that the Gr/Ni-foam exhibits the largest semi-circle arc, indicatives of the highest charge transfer resistance (8.83 Ω). This high resistance is attributed to incomplete Gr coverage, which permits the oxidation of the Ni-foam surface into insulating NiO (confirmed by XRD in Figure 2(f)), thereby hindering charge transfer. Notably, the growth of ZnO on Gr/Ni-foam significantly enhances charge transfer behavior, evidenced by the smaller semi-circle arc (Figure 3(b)). This improvement can be attributed to enhanced contact between ZnO and Gr/Ni-foam, resulting in lower interfacial resistance (Chen et al. 2015). While T-2 exhibits a low charge transfer resistance (1.06 Ω), it exhibits 87% decrease compared to the substrate, it is the T-8 sample that demonstrates the most optimized interface (Figure 3(c)). This is evidenced by a lower series resistance between the substrate and the active material, as indicated by its starting point closer to zero on the Nyquist plot.

Furthermore, the quantitative charge transfer resistance values further elucidate the influence of morphology on interfacial charge transfer. Specifically, T-8 exhibits a lower charge transfer resistance (1.67 Ω) compared with T-4 (1.88 Ω) and T-6 (2.31 Ω), indicating that the transition to the thin, interconnected flake-like morphology in T-8 reduces the kinetic barrier. Although T-10 shows a lower charge transfer resistance (1.65 Ω), the superior photocurrent density of T-8 highlights its optimized architecture that ensures efficient electrolyte accessibility and rapid charge transfer. Consequently, the reduced series and charge transfer resistance in T-8 contribute significantly to its enhanced PEC performance, demonstrating its potential as a promising photoelectrode for efficient H_2 evolution reaction. Given the excellent PEC activity of the T-8, it will be used as the basis for further investigation of the hydrothermal reaction temperature.

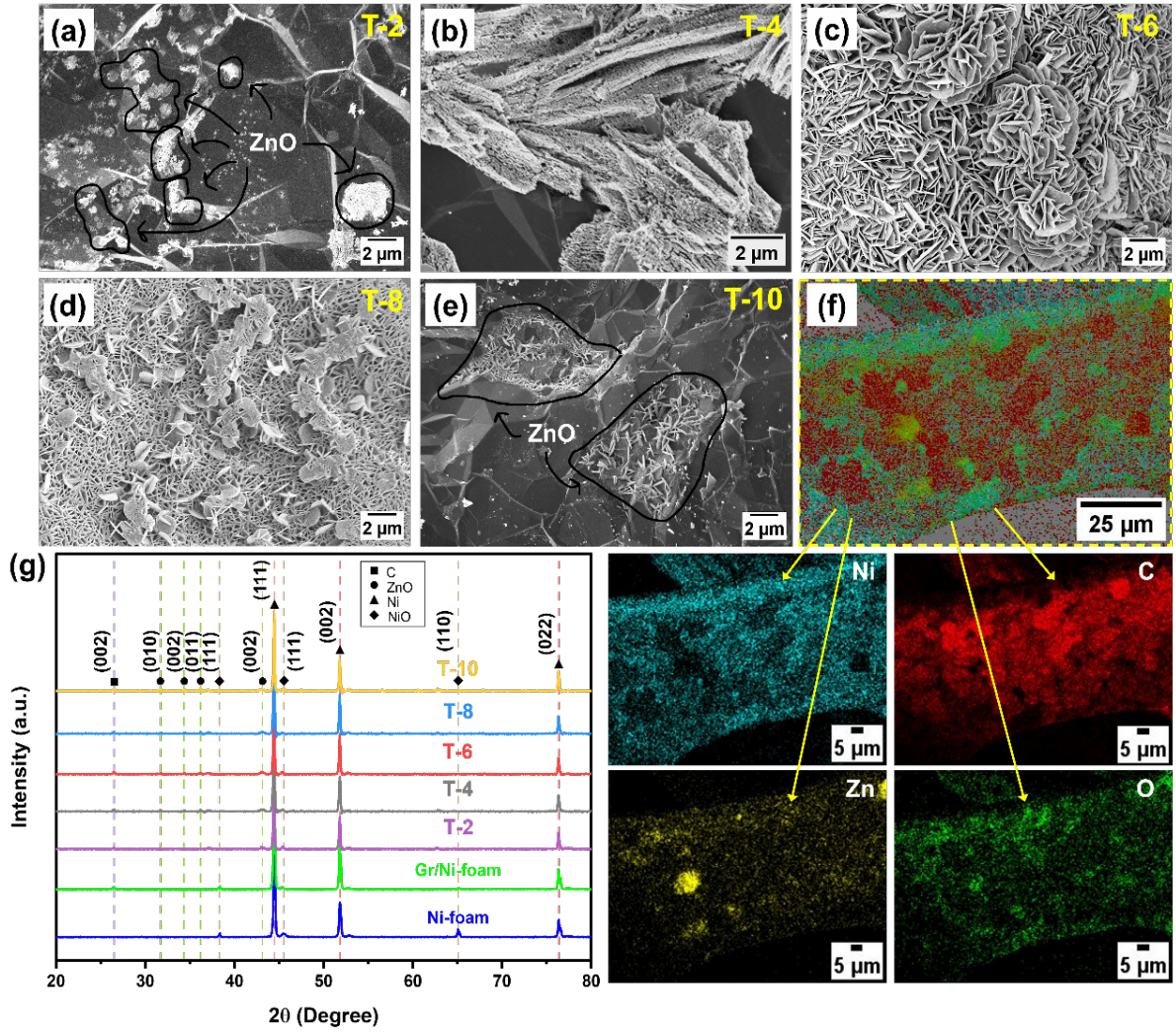

FIGURE 2. FESEM images of ZnO on Gr/Ni-foam at various hydrothermal time (a) 2, (b) 4, (c) 6, (d) 8, and (e) 10 h (all images were captured at the same magnification), (f) EDX mapping of T-2 and (g) XRD patterns of the as-synthesized samples

TABLE 1. PEC activities of different ZnO structures

Materials	Method	Morphologies of ZnO structures	Photocurrent densities (mA cm^{-2} vs Ag/AgCl)	References
ZnO/ITO	Dip coating, Hydrothermal	Nanorod	0.19 at 1 V	Mohd Fudzi et al. (2018)
ZnO/ITO	Radio frequency magnetron sputtering	Nanoflake	0.005 at 0.4 V	Sreedhar et al. (2019)
ZnO/ITO	Dip coating, Hydrothermal	Nanoflower	0.44 at 1 V	Holi, Ayal and Baqer (2019)
ZnO/Ni-foam	Hydrothermal	Nanorod	30.00 at 0.9 V	Gadisa et al. (2021)
ZnO/Ni-foam	Hydrothermal	Nanorod	17.18 at ~ 1 V	This work
ZnO/Gr/Ni-foam	CVD, Hydrothermal	Nanoflake	86.22 at ~1 V	This work

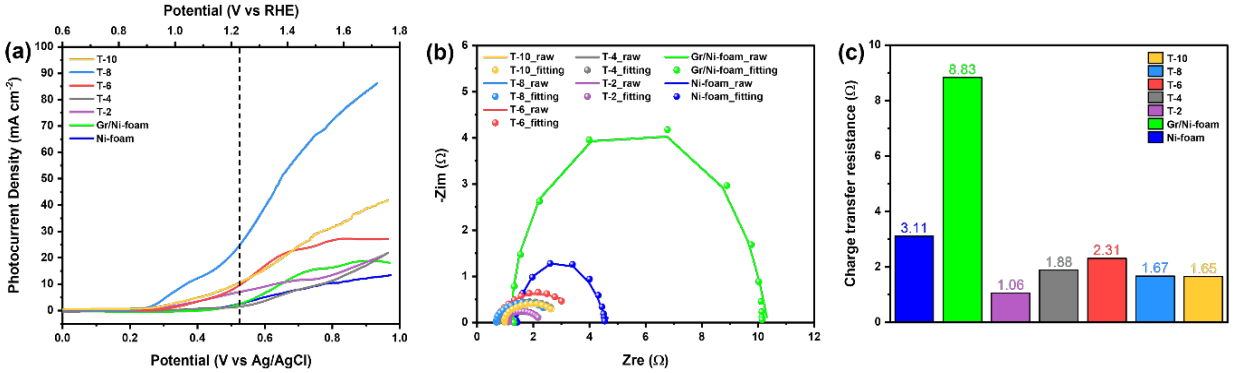

FIGURE 3. (a) Photocurrent activity, (b) Nyquist plot, and (c) Charge transfer resistance of synthesized samples

EFFECT OF HYDROTHERMAL REACTION TEMPERATURE ON ZnO GROWTH OVER Gr/Ni-FOAM SUBSTRATE

The morphological, structural, and PEC properties of ZnO on Gr/Ni-foam at different hydrothermal reaction temperatures were investigated using FESEM, XRD, and PEC activity, respectively. Figure 4 represents the FESEM images of the surface morphology of the ZnO on Gr/Ni-foam depending on the temperature. Initially, nanoflake ZnO were grown randomly on the Gr/Ni-foam at 150 ºC (Figure 4(a), 4(d) and Figure 2(d)). Then, increasing the temperature to 180 ºC led to the formation of the hexagonal structure at the flat ends of ZnO (Figure 4(b), 4(e)). As the reaction temperature increases to 200 ºC, the hexagonal structure of ZnO stacked up becomes a spherical structure (Figure 4(c), 4(f)). It can be concluded that the temperature affected the structure, coverage area and density of ZnO on Gr/Ni-foam. In addition, increasing the temperature through the use of NaOH can lead to a higher concentration of OH ions, which promotes the formation of $[Zn(OH)_4]^{2-}$ complexes and consequently influences the growth of ZnO (Edalati et al. 2016; Mohamed et al. 2019). Besides, the growth rate of ZnO increases at high temperatures, primarily due to increased interfacial reactions facilitated by higher activation energies, resulting in more rapid morphological changes (Raha & Ahmaruzzaman 2022).

Furthermore, the EDX mapping analysis of sample P-3 showed the existence and distribution of zinc (Zn), oxygen (O), C, and Ni elements in the scan area which further confirmed the successful growth of ZnO on Gr/Ni-foam during hydrothermal reaction (Figure 4(g)). This method produces high surface areas and offers more active sites using Ni-foam substrate (Gao et al. 2021; Zhang et al. 2012).

The information on the phase and crystallinity of ZnO on Gr/Ni-foam synthesized at different reaction temperatures was determined using an XRD (Figure 5(a)). The diffraction peaks of Ni were detected at 44.50°, 51.82°, and 76.32° for all samples, can be attributed to Ni-foam. In contrast, the crystal orientation of (002) at 26.44°, associated with graphitic carbon, decreased in intensity as the hydrothermal reaction temperature increased (Rosman et al. 2025). This could be ascribed to the high coverage area of the ZnO layer, which overlays the surface of Gr/Ni-foam. The hexagonal ZnO wurtzite structure was obtained, and the results agree closely with the values in the PDF number stated in previous section for peaks at 31.72° (010), 34.44° (002), 36.19° (011), 47.46° (012), 56.56° (110), 62.85° (013), 66.35° (020), 67.92° (112), 69.06° (021), and 77.02° (022). Similar findings have also been reported by Cai et al. (2016). The sharp and intense (011) peak ZnO at P-3 demonstrates high crystalline and high-density ZnO has grown along the yz-axis but not exactly perpendicular to the surface of Gr/Ni-foam, which could be attributed to the presence of Gr. Additionally, ZnO favored (011) orientation due to the reduction of internal stress and surface energy (Mohamed et al. 2019). The intensities of the ZnO peaks greatly increase with increasing reaction temperature, owing to the strain in the crystal lattice of ZnO with the high thermal energy supply, facilitating the migration of atoms to the suitable lattice position (Goswami, Adhikary & Bhattacharjee 2018; Koutu, Shastri & Malik 2017).

Figure 5(b) shows the PEC activity of ZnO on Gr/Ni-foam at different hydrothermal reaction temperatures. All samples exhibit a positive curve, indicating that the prepared samples are n-type semiconductors with electrons as the majority carriers, known as photoanodes (Abe 2010; Hossain et al. 2023). The high current is likely contributed by the porous structure of the Ni-foam substrate, which has good electrical conductivity (Su et al. 2021). Among the samples, P-3 demonstrates the highest photocurrent density followed by P-1 and P-2, with approximately 24.93, 16.10, and 12.87 cm mA^{-2} at 1.23 V vs RHE, respectively. This trend is consistent with the ABPE results (Rosman et al. 2025), where the P-3 sample achieves a maximum ABPE of 0.80% at 1.12 V vs RHE, which is 2.96 and 4.04 times higher than

P-1 and P-2, respectively, at 1.13 V vs RHE (Figure 5(c)). The superior PEC activity of P-3 could be attributed to the high crystallinity and coverage area of the well-defined hexagonal ZnO growth on the Gr/Ni-foam, as supported by FESEM and XRD analysis.

Notably, P-1 outperforms P-2 despite the higher thermal energy provided during the synthesis of P-2. This performance trend can be explained by the morphological transition of the ZnO, where P-1 maintains a high-surface-area nanoflake morphology that facilitates efficient charge transfer. In contrast, P-2 shows a transition toward bulkier hexagonal ZnO, which reduces the active surface area and increases the R2, as confirmed by the larger arc radius in the EIS results (Figure 5(d)). The arc radius of the semi-circular of P-3 is smaller than the arc radius of P-2 and P-1, indicating the rapid electron charge transfer with low resistance at the sample–electrolyte interface at higher temperature (Figure 5(d)). The equivalent circuit that fits the measured EIS result is tabulated in Table 2, where the Rs denoted the series resistance between the ZnO and Gr/Ni-foam substrate, R1 and R2 denote the charge transfer resistances within the sample and the sample–electrolyte interface, respectively, and CPE1 and CPE2 belong to the R1 and R2 dispersive resistance factors, respectively (Fareza, Nugroho & Fauzia 2022). Based on the CPE2 and R2 values, P-3 had the lowest internal resistance between sample–electrolyte interface among other samples, showing that this sample has high conductivity, which leads to better charge transfer and hence increases photocurrent density (Hayakawa et al. 2022; Saha, Gupta & Gómez García 2024). Therefore, the P-3 sample will be examined to acquire a better understanding.

EFFECT OF SUBSTRATE ON PEC ACTIVITY

To further understand the influence of the substrate, the PEC activity on Ni-foil was also examined and compared to the results obtained with Ni-foam. The graph in Figure 6 provides beneficial information, with ZnO on Gr/Ni-foam possessing the highest photocurrent density, followed by Gr/Ni-foam, ZnO/Ni-foam, Ni-foam, Gr/Ni-foil, ZnO on Ni-foil and Ni-foil. Interestingly, it confirmed that Ni-foam substrates outperformed Ni-foil in terms of PEC activity due to its porous nature, which provide an excellent interface between sample and electrolyte compared to non-porous substrate (Anuar et al. 2024; Liu et al. 2017). Furthermore, the photocurrent density of the sample on Ni-foam substrate continues to increase even at high positive voltage, possibly because

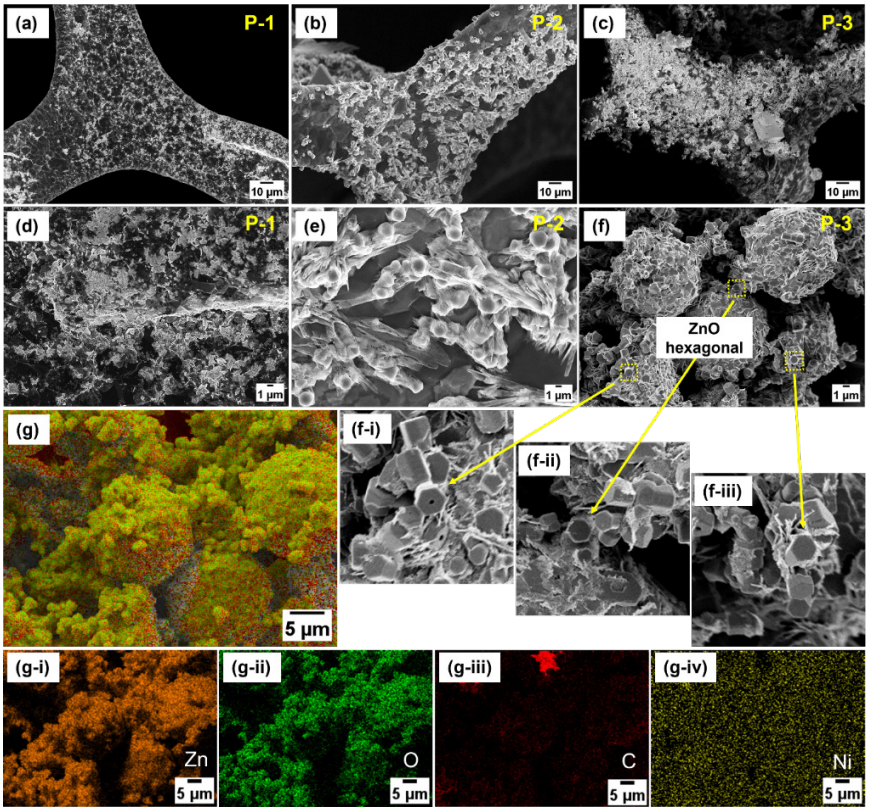

FIGURE 4. FESEM images of (a, d) P-1 (different magnification from FESEM image in Figure 2), (b, e) P-2, and (c, f) P-3 (ZnO hexagonal shape in f-i, f-ii, and f-iii), and (g) EDX elemental mapping images of sample P-3

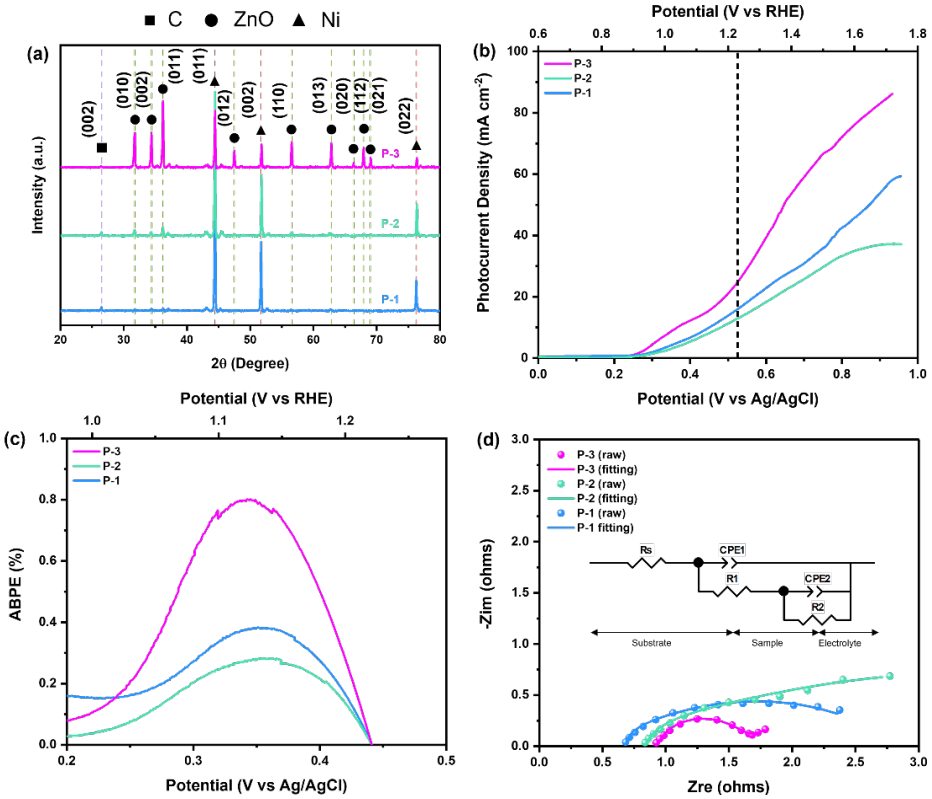

FIGURE 5. (a) XRD patterns, (b) Photocurrent density-potential curves, (c) ABPE curves, and (d) Nyquist plot obtained from EIS analysis with the equivalent circuit of ZnO on Gr/Ni-foam

TABLE 2. Impedance and photocurrent density of synthesized samples

Sample	Rs (Ω)	CPE1	R1 (Ω)	CPE2	R2 (Ω)	Photocurrent density (1.23 V vs RHE)
Ni-foam	1.38	-	-	6.95×10^{-5}	3.21	2.49
Gr/Ni-foam	1.35	4.68×10^{-5}	7.68×10^{-2}	2.87×10^{-5}	8.71	6.42
P-1	0.69	1.69×10^{-5}	4.33×10^{-7}	13.73×10^{2}	2.16	16.10
P-2	0.85	4.12×10^{-4}	1.93×10^{-7}	3.27×10^{2}	5.05	12.87
P-3	0.93	4.95×10^{-4}	6.63×10^{-1}	1.02×10^{-8}	1.80	24.93

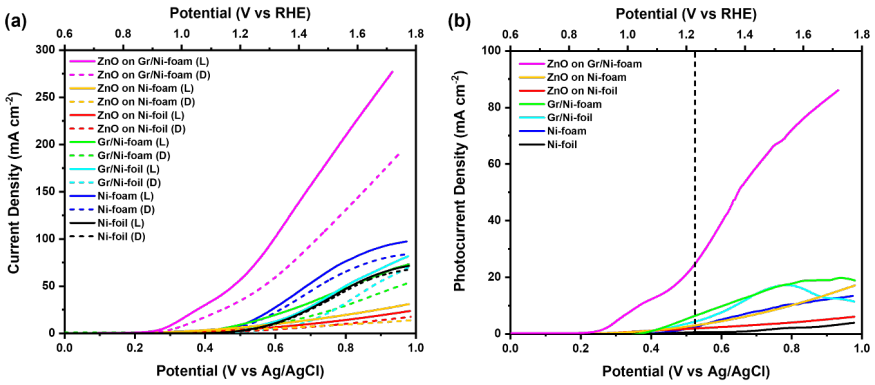

FIGURE 6. The PEC activity using Ni-foam and Ni-foil substrate (a) Current density-potential and (b) Photocurrent density-potential curve

of efficient charge transport and separation, resulting in effective rapid charge transfer. Besides, the onset potential shifted positively, from 0.6 V for Ni-foil and 0.4 V for Ni-foam to as low as 0.2 V for ZnO on Gr/Ni-foam. This near-zero onset potential highlights the role of Ni-foam substrate in facilitating water oxidation and confirms the photoanode characteristics of the ZnO on Gr/Ni-foam sample (Romeiro et al. 2017; Shinde et al. 2016). Beyond the structural advantages of the porous substrate, the use of Na_2SO_3 electrolyte as hole scavenger further enhances the PEC activity. The Na_2SO_3 effectively suppresses charge recombination by scavenging photogenerated holes, thereby reducing electron–hole recombination, promoting efficient charge transfer, and enhancing the overall PEC efficiency (Guo et al. 2018).

CONCLUSION

This study demonstrates that the introduction of Gr as a co-catalyst and Ni-foam as a porous substrate significantly enhances the PEC activity of ZnO. The morphology of ZnO growth on Gr/Ni-foam was successfully controlled by tuning the reaction time and temperature during the hydrothermal process, resulting in a highly crystalline structure ZnO was achieved, leading to improved PEC activity. Interestingly, the incorporation of Gr enhanced the charge transport property by reducing the onset potential. Not to mention, the porous structure of Ni-foam offers two key advantages: (a) improved light harvesting through increased light scattering and absorption, and (b) enhanced charge transfer due to larger surface area, facilitated charge transport within electrolyte, and reduced recombination of photogenerated electron–hole pairs during PEC reactions. It can be supported by experimental observations, with ZnO on Gr/Ni-foam exhibited a remarkable 9.6- and 29.35-times enhancement in photocurrent density compared to Ni-foam and Ni-foil, respectively, at 1.23 V vs RHE in 0.5 M Na_2SO_3. These findings highlight the potential of porous substrates for developing high-performance photoelectrodes for PEC applications.

ACKNOWLEDGEMENTS

This research was funded by Universiti Kebangsaan Malaysia (UKM) through a Research University Fund under the grant number (DIP-2019-020). We would also like to thank the Research and Instrumentation Management Center (CRIM), UKM for their technical assistance with this work.

REFERENCES

Abe, R. 2010. Recent progress on photocatalytic and photoelectrochemical water splitting under visible light irradiation. *Journal of Photochemistry and Photobiology C: Photochemistry Reviews* 11(4): 179-209. doi: 10.1016/j.jphotochemrev.2011.02.003

Anuar, N.A., Mohamed, M.A., Hasnan, N.S.N., Wan Mokhtar, W.N.A., Salehmin, M.N.I., Minggu, L.J. Mastuli, M.S. & Kassim, M.B. 2024. Porous architecture photoelectrode with boosted photoelectrochemical properties for solar fuel production. *International Journal of Hydrogen Energy* 51(PC): 476-507. doi: 10.1016/j.ijhydene.2023.10.098

Arifin, K., Yunus, R.M., Minggu, L.J. & Kassim, M.B. 2021. Improvement of TiO_2 nanotubes for photoelectrochemical water splitting: Review. *International Journal of Hydrogen Energy* 46(7): 4998-5024. doi: 10.1016/j.ijhydene.2020.11.063

Boruah, B.D., Mukherjee, A., Sridhar, S. & Misra, A. 2015. Highly dense ZnO nanowires grown on graphene foam for ultraviolet photodetection. *ACS Applied Materials and Interfaces* 7(19): 10606-10611. doi: 10.1021/acsami.5b02403

Cai, R., Wu, J.G., Sun, L., Liu, Y.J., Fang, T., Zhu, S., Li, S.Y., Wang, Y., Guo, L.F., Zhao, C.E. & Wei, A. 2016. 3D graphene/ZnO composite with enhanced photocatalytic activity. *Materials and Design* 90: 839-844. doi: 10.1016/j.matdes.2015.11.020

Chandrasekaran, S., Chung, J.S., Kim, E.J. & Hur, S.H. 2016. Exploring complex structural evolution of graphene oxide/ZnO triangles and its impact on photoelectrochemical water splitting. *Chemical Engineering Journal* 290: 465-476. doi: 10.1016/j.cej.2016.01.029

Chen, D., Wang, D., Ge, Q., Ping, G., Fan, M., Qin, L., Bai, L., Lv, C. & Shu, K. 2015. Graphene-wrapped ZnO nanospheres as a photocatalyst for high performance photocatalysis. *Thin Solid Films* 574: 1-9. doi: 10.1016/j.tsf.2014.11.051

Dias, P. & Mendes, A. 2019. Hydrogen production from photoelectrochemical water splitting. In *Fuel Cells and Hydrogen Production*, edited by Lipman, T.E. & Weber, A.Z. New York: Springer. pp. 1003-1053.

Edalati, K., Shakiba, A., Vahdati-Khaki, J. & Zebarjad, S.M. 2016. Low-temperature hydrothermal synthesis of ZnO nanorods: Effects of zinc salt concentration, various solvents and alkaline mineralizers. *Materials Research Bulletin* 74: 374-379. doi: 10.1016/j.materresbull.2015.11.001

Effendi, N.A.S., Samsi, N.S., Zawawi, S.A., Hassan, O.H., Zakaria, R., Yahya, M.Z.A. & Ali, A.M.M. 2017. Studies on graphene zinc-oxide nanocomposites photoanodes for high-efficient dye-sensitized solar cells. *AIP Conference Proceedings* 1877 (1): 090005. doi: 10.1063/1.4999900

Fareza, A.R., Nugroho, F.A.A. & Fauzia, V. 2022. One-step coating of a ZnS nanoparticle/MoS_2 nanosheet composite on supported ZnO nanorods as anodes for photoelectrochemical water splitting. *ACS Applied Nano Materials* 5(11): 16051-16060. doi: 10.1021/acsanm.2c01434

Gadisa, B.T., Appiah-Ntiamoah, R. & Kim, H. 2019. *In-situ* derived hierarchical ZnO/Zn-C nanofiber with high photocatalytic activity and recyclability under solar light. *Applied Surface Science* 491(February): 350-359. doi: 10.1016/j.apsusc.2019.06.159

Gadisa, B.T., Baye, A.F., Appiah-Ntiamoah, R. & Kim, H. 2021. ZnO@Ni foam photoelectrode modified with heteroatom doped graphitic carbon for enhanced photoelectrochemical water splitting under solar light. *International Journal of Hydrogen Energy* 46(2): 2075-2085. doi: 10.1016/j.ijhydene.2020.10.094

Gaidi, M., Salem, M., Akir, S., Massoudi, I., Ghrib, T., Litaiem, Y. & Khirouni, K. 2018. ZnO and carbon nanocomposites for enhanced photoelectrochemical sensing activity: Influence of the carbon content. *Journal of Solid State Electrochemistry* 22(11): 3631-3637. doi: 10.1007/s10008-018-4062-4

Gao, C., Zhong, K., Fang, X., Fang, D., Zhao, H., Wang, D., Li, B., Zhai, Y., Chu, X., Li, J. & Wang, X. 2021. Brief review of photocatalysis and photoresponse properties of ZnO–graphene nanocomposites. *Energies* 14(19): 6403. doi: 10.3390/en14196403

Geim, A.K. & Novoselov, K.S. 2007. The rise of graphene. *Nature Materials* 6(3): 183-191. doi: 10.1038/nmat1849

Goswami, M., Adhikary, N.C. & Bhattacharjee, S. 2018. Effect of annealing temperatures on the structural and optical properties of zinc oxide nanoparticles prepared by chemical precipitation method. *Optik* 158: 1006-1015. doi: 10.1016/j.ijleo.2017.12.174

Guo, S., Zhao, X., Zhang, W. & Wang, W. 2018. Optimization of electrolyte to significantly improve photoelectrochemical water splitting performance of ZnO nanowire arrays. *Materials Science and Engineering B: Solid-State Materials for Advanced Technology* 227(June 2017): 129-135. doi: 10.1016/j.mseb.2017.09.020

Hayakawa, E., Nakamura, H., Ohsaki, S. & Watano, S. 2022. Characterization of solid-electrolyte/active-material composite particles with different surface morphologies for all-solid-state batteries. *Advanced Powder Technology* 33(3): 103470. doi: 10.1016/j.apt.2022.103470

Holi, A.M., Ayal, A.K. & Baqer, A.A. 2019. Construction of ZnO-nanoflowers photoanode for photoelectrochemical cell. *Journal of Physics: Conference Series* 1234: 012056. doi: 10.1088/1742-6596/1234/1/012056

Hong, X., Wang, X., Li, Y., Fu, J. & Liang, B. 2020. Progress in graphene/metal oxide composite photocatalysts for degradation of organic pollutants. *Catalysts* 10(8): 921. doi: 10.3390/catal10080921

Hossain, N., Mobarak, M.H., Mimona, M.A., Islam, M.A., Hossain, A., Zohura, F.T. & Chowdhury, M.A. 2023. Advances and significances of nanoparticles in semiconductor applications - A review. *Results in Engineering* 19(August): 101347. doi: 10.1016/j.rineng.2023.101347

Jung, M.H. & Chu, M.J. 2014. Synthesis of hexagonal ZnO nanodrums, nanosheets and nanowires by the ionic effect during the growth of hexagonal ZnO crystals. *J. Mater. Chem. C*. 2(32): 6675-6682. doi: 10.1039/C4TC01132E

Karimizadeh, N., Babamoradi, M., Azimirad, R. & Khajeh, M. 2018. Synthesis of three-dimensional multilayer graphene foam/ZnO nanorod composites and their photocatalyst application. *Journal of Electronic Materials* 47(9): 5452-5457. doi: 10.1007/s11664-018-6427-y

Koutu, V., Shastri, L. & Malik, M.M. 2017. Effect of temperature gradient on zinc oxide nano particles synthesized at low reaction temperatures. *Materials Research Express* 4: 035011. doi: 10.1088/2053-1591/aa5855

Li, C.H., Li, M.C., Liu, S.P., Jamison, A.C., Lee, D., Lee, T.R. & Lee, T.C. 2016. Plasmonically enhanced photocatalytic hydrogen production from water: The critical role of tunable surface plasmon resonance from gold-silver nanoshells. *ACS Applied Materials and Interfaces* 8(14): 9152-61. doi: 10.1021/acsami.6b01197

Liu, T., Ding, J., Su, Z. & Wei, G. 2017. Porous two-dimensional materials for energy applications: Innovations and challenges. *Materials Today Energy* 6: 79-95. doi: 10.1016/j.mtener.2017.08.006

Macclesh del Pino Pérez, L.A., Morales Cepeda, A.B., García Alamilla, R., Rivera Armenta, J.L. & Sanches Valdéz, S. 2019. Nanostructures of graphene oxide modified with ZnO: Synthesis and photocatalyst evaluation under sunlight. *Fullerenes Nanotubes and Carbon Nanostructures* 27(8): 632-639. doi: 10.1080/1536383X.2019.1627522

Mahmud, R.A., Shafawi, A.N., Ahmed Ali, K., Putri, L.K., Md Rosli, N.I. & Mohamed, A.R. 2020. Graphene nanoplatelets with low defect density as a synergetic adsorbent and electron sink for ZnO in the photocatalytic degradation of methylene blue under UV–Vis irradiation. *Materials Research Bulletin* 128(March): 110876. doi: 10.1016/j.materresbull.2020.110876

Megia, P.J., Vizcaino, A.J., Calles, J.A. & Carrero, A. 2021. Hydrogen production technologies: From fossil fuels toward renewable sources. A mini review. *Energy and Fuels* 35(20): 16403-16415. doi: 10.1021/acs.energyfuels.1c02501

Men, X., Chen, H., Chang, K., Fang, X., Wu, C., Qin, W. & Yin, S. 2016. Three-dimensional free-standing ZnO/graphene composite foam for photocurrent generation and photocatalytic activity. *Applied Catalysis B: Environmental* 187: 367-374. doi: 10.1016/j.apcatb.2016.01.052

Mohamed, M.A.M., Zain, M.F., Jeffery Minggu, L., Kassim, M.B., Jaafar, J., Saidina Amin, N.A., Mastuli, M.S., Wu, H., Wong, R.J. & Ng, Y.H. 2019. Bio-inspired hierarchical hetero-architectures of *in-situ* C-doped g-C_3N_4 grafted on C, N Co-doped ZnO micro-flowers with booming solar photocatalytic activity. *Journal of Industrial and Engineering Chemistry* 77: 393-407. doi: 10.1016/j.jiec.2019.05.003

Mohamed Saheed, M.S., Mohamed, N.M., Mahinder Singh, B.S., Wali, Q., Saheed, M.S.M. & Jose, R. 2021. Foam-like 3D graphene as a charge transport modifier in zinc oxide electron transport material in perovskite solar cells. *Photochem*. 1(3): 523-536. doi: 10.3390/photochem1030034

Mohd Fudzi, L., Zainal, Z., Lim, H.N., Chang, S.K., Holi, A.M. & Sarif@Mohd Ali, M. 2018. Effect of temperature and growth time on vertically aligned ZnO nanorods by simplified hydrothermal technique for photoelectrochemical cells. *Materials* 11(5): 704. doi: 10.3390/ma11050704

Mohd Shah, N.R.A., Rosman, N.N., Wong, W.Y., Arifin, K., Jeffery Minggu, L. & Mohamad Yunus, R. 2022a. Effect of annealing time on chemical vapor deposition growth of 3D graphene for photoelectrochemical water splitting. *Materials Today: Proceedings* 57: 1215-1219. doi: 10.1016/j.matpr.2021.11.024

Mohd Shah, N.R.A., Yunus, R.M., Rosman, N.N., Wong, W.Y., Arifin, K. & Minggu, L.J. 2022b. Synthesis of ZnO on 3D graphene/nickel foam for photoelectrochemical water splitting. *Malaysian Journal of Analytical Sciences* 26(3): 546-553.

Mohd Shah, N.R.A., Mohamad Yunus, R., Rosman, N.N., Wong, W.Y., Arifin, K. & Jeffery Minggu, L. 2021. Current progress on 3D graphene-based photocatalysts: From synthesis to photocatalytic hydrogen production. *International Journal of Hydrogen Energy* 46(14): 9324-9340. doi: 10.1016/j.ijhydene.2020.12.089

Moridon, S.N.F., Salehmin, M.I., Mohamed, M.A., Arifin, K., Minggu, L.J. & Kassim, M.B. 2019. Cobalt oxide as photocatalyst for water splitting: Temperature-dependent phase structures. *International Journal of Hydrogen Energy* 44(47): 25495-25504. doi: 10.1016/j.ijhydene.2019.08.075

Nordin, N., Adris, N.A., Minggu, L.J., Arifin, K., Yunus, R.M., Mohamed, M.A., Timmiati, S.N., Yin, W.W. & Kassim, M.B. 2025. Comparison of photoelectrochemical activities of nickel metal foam after heat treatment and coated with Fe_2O_3 for water molecule splitting applications. *Sains Malaysiana* 54(2): 505-515. doi: 10.17576/jsm-2025-5402-16

Ong, C.B., Ng, L.Y. & Mohammad, A.W. 2018. A review of ZnO nanoparticles as solar photocatalysts: Synthesis, mechanisms and applications. *Renewable and Sustainable Energy Reviews* 81: 536-551. doi: 10.1016/j.rser.2017.08.020

Pirhashemi, M., Habibi-Yangjeh, A. & Rahim Pouran, S. 2018. Review on the criteria anticipated for the fabrication of highly efficient ZnO-based visible-light-driven photocatalysts. *Journal of Industrial and Engineering Chemistry* 62: 1-25. doi: 10.1016/j.jiec.2018.01.012

Pratomo, U., Pratama, R.A., Irkham, I., Sulaeman, A.P., Mulyana, J.Y. & Primadona, I. 2023. 3D-ZnO superstructure decorated with carbon-based material for efficient photoelectrochemical water-splitting under visible-light irradiation. *Nanomaterials* 13(8): 1380. doi: 10.3390/nano13081380

Pruna, A., Wu, Z., Zapien, J.A., Li, Y.Y. & Ruotolo, A. 2018. Enhanced photocatalytic performance of ZnO nanostructures by electrochemical hybridization with graphene oxide. *Applied Surface Science* 441: 936-944. doi: 10.1016/j.apsusc.2018.02.117

Qian, H., Liu, Z., Zhang, B., Li, J. & Ya, J. 2021. Optimized the carrier transport path and separation efficiency of 2D/2D heterojunction in photoelectrochemical water splitting. *ChemCatChem* 13(8): 1940-1950. doi: 10.1002/cctc.202001765

Qiu, B., Xing, M. & Zhang, J. 2018. Recent advances in three-dimensional graphene based materials for catalysis applications. *Chemical Society Reviews* 47(6): 2165-2216. doi: 10.1039/c7cs00904f

Raha, S. & Ahmaruzzaman, M. 2022. ZnO nanostructured materials and their potential applications: Progress, challenges and perspectives. *Nanoscale Advances* 4(8): 1868-1925. doi: 10.1039/D1NA00880C

Raizada, P., Sudhaik, A. & Singh, P. 2019. Photocatalytic water decontamination using graphene and ZnO coupled photocatalysts: A review. *Materials Science for Energy Technologies* 2(3): 509-525. doi: 10.1016/j.mset.2019.04.007

Romeiro, F.C., Rodrigues, M.A., Silva, L.A.J., Catto, A.C., Silva, L.F., da Longo, E., Nossol, E. & Lima, R.C. 2017. RGO-ZnO nanocomposites for high electrocatalytic effect on water oxidation obtained by microwave-hydrothermal method. *Applied Surface Science* 423: 743-751. doi: 10.1016/j.apsusc.2017.06.221

Rosman, N.N., Mohd Shah, N.R.A., Moridon, S.N.F., Arifin, K., Jeffery Minggu, L., Ahmad Ludin, N. & Mohamad Yunus, R. 2025. *In situ* formation of ZnS/Ni_3S_2 with hybrid nanostructure of MoS_2/ZnO on graphene/nickel foam for enhanced photoelectrochemical activity. *International Journal of Hydrogen Energy* 104 (February): 324-335. doi: 10.1016/j.ijhydene.2024.06.204

Rosman, N.N., Mohamad Yunus, R., Jeffery Minggu, L., Arifin, K., Kassim, M.B. & Mohamed, M.A. 2021. Vertical MoS_2 on SiO_2/Si and graphene: Effect of surface morphology on photoelectrochemical properties. *Nanotechnology* 32(3): 035705. doi: 10.1088/1361-6528/abbea9

Saha, R., Gupta, K. & Gómez García, C.J. 2024. Strategies to improve electrical conductivity in metal–organic frameworks: A comparative study. *Crystal Growth & Design* 24(5): 2235-2265. doi: 10.1021/acs.cgd.3c01162

Seravalli, L. & Bosi, M. 2021. A review on chemical vapour deposition of two-dimensional MoS_2 flakes. *Materials* 14(24): 7590. doi: 10.3390/ma14247590

Shaker, L.M., Mohammed, J.K., Basem, A., Halbos, R.J., Mahdi, R.R., Mohammed, S.A., Fayad, M.A., Al-Amiery, A. & Al Lami, M.H. 2024. Comparative analysis of solar cells and hydrogen fuel: A mini-review. *Results in Engineering* 23(June): 102507. doi: 10.1016/j.rineng.2024.102507

Shinde, P.S., Choi, S.H., Kim, Y., Ryu, J. & Jang, J.S. 2016. Onset potential behavior in α-Fe_2O_3 photoanodes: The influence of surface and diffusion Sn doping on the surface states. *Physical Chemistry Chemical Physics* 18(4): 2495-2509. doi: 10.1039/C5CP06669G

Sohaib, M., Iqbal, T., Afsheen, S., Tahir, M.B., Masood, A., Rafique, M., Riaz, K.N., Sayed, M.A., Abd El-Rehim, A.F. & Ali, A.M. 2023. Novel sol–gel synthesis of Mo-doped ZnO-NPs for photo-catalytic waste water treatment using the RhB dye as a model pollutant. *Environment, Development and Sustainability* 25(10): 11583-11598. doi: 10.1007/s10668-022-02543-9

Sreedhar, A., Neelakanta Reddy, I., Ta, Q.T.H., Namgung, G. & Noh, J. 2019. Plasmonic Ag nanowires sensitized ZnO flake-like structures as a potential photoanode material for enhanced visible light water splitting activity. *Journal of Electroanalytical Chemistry* 832: 426-435. doi: 10.1016/j.jelechem.2018.11.042

Su, L., Zhan, J., Gu, Q., Chen, H., Wang, L., Wang, Y., Hu, Q. & Ren, M. 2021. N-doped carbon nanolayer modified nickel foam: A novel substrate for supercapacitors. *Applied Surface Science* 546(October 2020): 148754. doi: 10.1016/j.apsusc.2020.148754

Xu, T., Zhang, L., Cheng, H. & Zhu, Y. 2011. Significantly enhanced photocatalytic performance of ZnO via graphene hybridization and the mechanism study. *Applied Catalysis B: Environmental* 101(3-4): 382-387. doi: 10.1016/j.apcatb.2010.10.007

Yang, F., Cao, B., Tao, Y., Hu, M., Feng, C., Wang, L., Jiang, Z., Cao, D. & Zhang, Y. 2015. Electrodeposition of palladium on carbon nanotubes modified nickel foam as an efficient electrocatalyst towards hydrogen peroxide reduction. *Journal of Power Sources* 298: 38-45. doi: 10.1016/j.jpowsour.2015.08.052

Yusoff, N., Ho, L.N., Ong, S.A., Wong, Y.S., Khalik, W. & Ridzwan, M.F. 2017. Enhanced photodegradation of phenol by ZnO nanoparticles synthesized through sol-gel method. *Sains Malaysiana* 46(12): 2507-2514. doi: 10.17576/jsm-2017-4612-28

Zhang, Y., Ram, M.K., Stefanakos, E.K. & Goswami, D.Y. 2012. Synthesis, characterization, and applications of ZnO nanowires. *Journal of Nanomaterials* 2012(1): 624520. doi: 10.1155/2012/624520

*Corresponding author; email: rozanyunus@ukm.edu.my